Fabrication and Performance of Atmospheric Plasma Sprayed Solid Oxide Fuel Cells with Liquid Antimony Anodes

Yidong Jiang
Department of Energy and Power Engineering, Tsinghua University https://orcid.org/0000-0003-0633-1399

Wenfei Mo
Department of Energy and Power Engineering, Tsinghua University

Tianyu Cao
Chemical and Biomolecular Engineering, University of Pennsylvania

Yixiang Shi (shyx@tsinghua.edu.cn)
https://orcid.org/0000-0001-8720-9699

Ningsheng Cai
Department of Energy and Power Engineering, Tsinghua University

Research

Keywords: Solid Oxide Fuel Cells, Liquid Antimony Anodes, Atmospheric Plasma Spraying

Posted Date: October 14th, 2020

DOI: https://doi.org/10.21203/rs.3.rs-45968/v2

Version of Record: A version of this preprint was published at International Journal of Coal Science & Technology on April 30th, 2021. See the published version at https://doi.org/10.1007/s40789-021-00430-8.

Abstract

A Solid oxide fuel cell (SOFC) with a liquid antimony anode (LAA) is a potential energy conversion technology for impurity-containing fuels. Atmospheric plasma spraying (APS) technology has become a promising LAA-SOFC preparation method because of its economy and convenience. In this paper, button SOFCs with different cathode materials and ratios of pore former were prepared by the APS method and measured at 750°C. The effect of the cathode structure on the electrochemical performance of the LAA-SOFCs was analyzed, and an optimized spraying method for LAA-SOFCs was developed. A tubular LAA-SOFC was prepared by the APS method based on the optimized spraying method and a peak power of 2.5 W was reached. The tubular cell was also measured at a constant current of 2 A for 20 hours and fed with a sulfur-containing fuel to demonstrate its impurity resistance and electrode stability.

Introduction

Solid carbon fuels are widely utilized due to their high yield and low price (Wall 2005). However, solid carbon fuels have obvious disadvantages when they are employed in fuel cells, such as the severe contact between solid carbon particles and solid anodes, limited fuel transportation in the anode reaction chamber, and complex poisoning of carbon fuels (Cao et al. 2017; Wang et al. 2014c). Integrated gasification fuel cell (IGFC) technology combines electrochemical reactions with thermal cycles for power generation, thereby realizing the indirect electrochemical utilization of coal and greatly improving the efficiency of coal power generation (Dong et al. 2019; Li et al. 2010).

In an IGFC system, the coals are first converted into syngas (mainly consisting of CO, H_2, CO_2 and CH_4) by a flowing gasifying agent (Li et al. 2014). The generated syngas is sent into the purification unit for desulfurization and dedusting. Then, the purified syngas is fed into the anode chamber of the high-temperature solid oxide fuel cells (SOFCs), where the syngas reacts with the oxygen ions from the cathode (Fan and Han 2014). In fuel cells, most of the combustible components in syngas are converted into electricity and heat by particular reactions. The unconverted syngas is then sent to the combustion furnace for power generation via a thermal cycle.

Liquid metal anode SOFCs are a promising technology for converting fuels containing sulfur and ash. With liquid metal anodes, the cost for impurity removal in IGFC systems can be reduced. To find suitable liquid metal anode materials with decent electrochemical performance for SOFCs, Sn (Tao et al. 2007; Wang et al. 2014b), Sb (Duan et al. 2016; Jayakumar et al. 2011), Ag (Javadekar et al. 2012) and Bi (Jayakumar et al. 2010) have been previously studied. Antimony (Sb) is an attractive choice for liquid metal anodes. Compared to Bi (0.45 V at 700°C) and Ag (0.3 V), the liquid antimony anode (LAA) has an adequate open-circuit voltage (0.75 V). Furthermore, the melting points of Sb (630°C) and its oxide (Sb_2O_3, 656°C) are more easily attained. In contrast, the product of Sn oxidation (SnO_2) has a melting point of 1630°C, which impedes further electrochemical reactions (Wang et al. 2014b). Jayakumar et al. (2011) developed an SOFC with an LAA. The working principle of the LAAs is shown in Figure 1. If syngas is used as the fuel, the circular reactions in the LAAs are represented as:

See equations 1 and 2 in the supplementary files.

Since the density of Sb_2O_3 is less than Sb, the Sb_2O_3 generated at the anode-electrolyte interface by Eq. 1 can float to the surface of the LAA. Once the floating Sb_2O_3 is reduced to metallic antimony by the fuels via Eq. 2, the generated antimony will sink to the electrochemical reaction region due to its high density. This reaction cycle between Sb_2O_3 and Sb enables the fuel cell to continuously operate and avoids the impact of ash on the SOFC performance. The relatively large amount of anode materials (more than 10 g of antimony per cm^2 reaction area in the current research) keeps the electrochemical performance of the SOFC stable even if part of the liquid metal reacts with the sulfur that is present in the fuels (Jiang et al. 2020). In our previous studies, the kinetics of the anode-electrolyte interfacial reactions and the antimony oxidation process were analyzed (Wang et al. 2013; Wang et al. 2014c). A tubular LAA-SOFC was also measured, showing it had potential for an expanded reaction area (Cao et al. 2019). However, significant hot corrosion on the sintered electrolyte by liquid antimony had been observed in previous research (Jayakumar et al. 2013; Ma et al. 2019). Therefore, the fabrication of corrosion-proof electrolytes is of crucial importance.

Atmospheric plasma spraying (APS) is a widely adopted surface layer preparation technology used in the preparation of thermal barrier coatings and surface protection layers. The APS method can prepare SOFCs by depositing cell components on porous metal or cermet supports (Henne 2007; Zhang et al. 2017). In addition, the electrolyte layer prepared by the APS method can effectively resist the corrosion of liquid metal and its oxides, which suggests that APS is a potential method to prepare durable electrolytes for LAA-SOFCs (Cao et al. 2018). For most of the plasma-sprayed SOFCs, the anodes were deposited on the support and the cathodes were prepared at the outermost layer of the cell. However, in regard to LAA-SOFCs, the cathodes should be prepared between the support and electrolyte because the LAA cannot stay stable between these two layers. These types of electrode arrangement methods are termed anode-down and cathode-down, respectively (Metcalfe et al. 2013). In previous studies (Cao et al. 2019; Waldbillig and Kesler 2011), the polarization impedance of the plasma-sprayed cathode-down fuel cells was relatively large, and the ex situ characterization showed the cathodes had a low porosity. The porosity could be increased by preparing the cathodes with a low torch power and long spray distance. Nevertheless, the bond strength of the cathode decreased, which made the coating crack or break off in the subsequent electrolyte preparation of the cathode-down cells. Therefore, the cathode porosity should be improved by other methods, such as adding a pore former into the cathode powder. Carbon black is a popular pore former in cathode preparation of the plasma-sprayed anode-down SOFCs because of its high melting point and decent oxidizability. Tsai et al. (2014) prepared an APS LSCF-LSGM ($La_{0.58}Sr_{0.4}Co_{0.2}Fe_{0.8}O_{3-\delta}$–$La_{0.8}Sr_{0.2}Ga_{0.8}Mg_{0.2}O_{3-\delta}$) composite cathode with a polarization resistance of 0.128 Ω cm^2 at 750°C. The cathode was deposited at the outermost layer with 15 wt.% carbon black as a pore former. Harris et al. (2017) prepared the LSCF-SDC ($La_{0.6}Sr_{0.4}Co_{0.2}Fe_{0.8}O_{3-\delta}$–$Ce_{0.8}Sm_{0.2}O_{1.9}$) cathodes by the APS method. In their research, 25 wt.% carbon black was employed as a pore former and the polarization resistance was 0.37 Ω cm^2 at 750°C. However, for the cathode-down plasma-sprayed SOFCs, the ratio of pore former in the cathode powder still needs to be optimized.

In this paper, button LAA-SOFCs with different cathode materials and ratios of pore former were prepared by the APS method and were tested at 750°C. The effect of the cathode structure on the electrochemical performance of the cathode-down APS fuel cells was analyzed, and an optimized spraying method for the cathodes of the cathode-down APS fuel cells was developed. A tubular LAA-SOFC was prepared by the APS method based on the optimized spraying method. The tubular LAA-SOFC was measured for 20 hours with a sulfur-containing fuel to demonstrate the stability of the electrodes.

Experimental Preparation

Two configurations of the LAA-SOFCs were prepared and characterized in this study. Button fuel cells (25 mm*25 mm*1.8 mm) were prepared for optimizing the coating manufacturing process, and the tubular fuel cell (diameter: 25 mm, length: 200 mm) was prepared for enlargement. The preparation and characterization methods of the two configurations of the LAA-SOFCs are described below.

2.1. APS Button LAA-SOFC Preparation and Characterization

The plasma-sprayed cathodes and electrolyte of the LAA-SOFC used for the present research were prepared on stainless steel substrates. The manufacturing methods for stainless steel substrates with a porosity of 20 ± 2% were discussed in our previous work (Cao et al. 2019).

For the button fuel cells, porous cathodes were deposited on stainless steel substrates by the APS (Zhen-Bang Aerospace Precision Machinery Co., Ltd., China) method. The cathode powder (LSCF, $La_{0.6}Sr_{0.4}Co_{0.2}Fe_{0.8}O_{3-\delta}$, Qingdao Tianyao Materials Co., Ltd., China) used for cathode spraying contained 15, 10, 5 and 0 wt. % carbon black as the pore former to make the cathode layer porous. These cells are hereinafter referred to as LSCF10, LSCF5 and LSCF0. LSM ($La_{0.8}Sr_{0.2}MnO_{3-\delta}$, Qingdao Tianyao Materials Co., Ltd., China) powder with 10 wt.% carbon black was also used for spraying as a control group to evaluate the difference in cathodes. It is hereinafter referred to as LSM10. The thicknesses of the cathodes were all approximately 20 μm. The electrolyte was prepared by the same APS system as the cathodes. The powder used for electrolyte spraying was 8YSZ (8 mol% Y_2O_3-ZrO_2, Qingdao Tianyao Materials Co., Ltd., China), and the thickness of the electrolyte was approximately 100 μm. Other parameters of the APS method are listed in Table 1.

Table 1

Atmospheric plasma spraying parameters.

Parameters	Value of cathode	Value of electrolyte	Unit
Torch power	30	45	kW
Torch current	550	700	A
Flow rate of Ar	50	45	slpm
Flow rate of H_2	0	5	slpm
Spray distance	110	80	mm
Powder feed rate	25	10	g min^{-1}

The testing setup used for the sprayed button cells was mentioned in our previous research (Jiang et al. 2019). The electrochemical performances of the button cells were measured by the four-probe method with an electrochemical workstation (IM6ex, Zahner-Elektrik GmbH, Germany). The LAA-SOFCs should be operated at higher than 656℃ (the melting point of the Sb_2O_3) to protect the anode-electrolyte interface from the Sb_2O_3 deposition. Meanwhile, the LAA-SOFC with the SUS430 support could not be operated at higher than 800℃ because the support was set at the cathode side and the stainless steel would be rapidly oxidized at such temperature. Therefore, the present LAA-SOFCs were only suitable for operating at 700℃ or 750℃ and we tested the cells at 750℃ in the present study for a decent performance. The polarization curves of the cells were measured at a speed of 10 mV s^{-1}, and the finishing test voltage was 0.2 V. The electrochemical impedance spectra (EIS) of the cells were all measured at open-circuit voltage. The amplitude during the EIS testing was 20 mV, and the frequency ranged from 100 kHz to 0.1 Hz. In the experiments of the button cells, an Ar gas flow was fed into the anode chamber at a flow rate of 20 sccm, and at the cathode side, oxygen was provided by convection in the furnace. No fuel was supplied during the experiments. An optimized preparation method was chosen by measuring the electrochemical performance of the button cells with different cathodes.

After the tests, the button cells were removed from the reactors, cut vertically, fixed in an epoxy mold and then polished by abrasive paper for scanning electron microscopy (SEM). The sample was then characterized by SEM (Zeiss Merlin VP compact, Germany) to obtain cross-sectional images of the fuel cells.

2.2. APS Tubular LAA-SOFC Preparation and Characterization

The tubular fuel cell was prepared by the same stainless steel substrate manufacturing and APS method as the button cells. The optimized preparation method from the button cell experiments was used for preparing the cathode of the tubular cell, and the thicknesses of the cathode and electrolyte were consistent with those of the button fuel cells.

The setup for the tubular fuel cell is shown in Figure 2. An SUS430 stainless steel tube was connected to the metal support of the tubular fuel cell as both the current collector and air channel. Then, 1500 g of

antimony powder (500 mesh, Changsha Tianjiu Metal Material Co., Ltd., China) was loaded into an alumina crucible. The crucible was then fixed in a vertical tube furnace and heated to 750°C for 10 hours. An Ar gas flow was fed into the crucible during the heating process at a rate of 100 sccm (standard-state cubic centimeter per minute) to prevent the antimony from being oxidized, and an air flow was fed into the tubular cell at a flow rate of 100 sccm. After the antimony was completely melted, the fuel cell was inserted into the liquid antimony bath at a speed of approximately 0.1 cm s^{-1} until the cell touched the bottom of the crucible. The calculated depth of the liquid antimony bath was 7.6 cm. Two graphite rods were employed for current collection at the anode, and the rods were mainly shielded in alumina tubes to avoid oxidation by the antimony oxide.

The electrochemical performances of the tubular cell were measured by the same electrochemical workstation as the button cells at 750°C. The polarization curves and EIS were also measured by the same methods as the button cells. Constant current discharging was measured with the tubular cell at a current of 2 A for 20 hours. During the tubular cell experiment, the flow rates were 50 sccm for the Ar flow and 400 sccm for the air flow. Taixi deashed anthracite coal (Shenhua Ningxia Coal Industry Group Co., Ltd, China) was supplied to the antimony bath as the fuel. Ten grams of coal was added to the anode chamber at the beginning of the constant current test and 10 hours after the test began. The tubular cell was pulled out from the liquid antimony bath at a speed of approximately 0.1 cm s^{-1} after all of the tests were finished.

Results And Discussion

3.1 Performance of the Button LAA-SOFC

Figure 3 (a) and (b) show the polarization curves and the EIS results, respectively, of the LSCF cathode button fuel cells with different amounts of pore former. The LSCF10 cell reached the peak power density of 70 mW cm^{-2}, and the peak power densities of the LSCF5 and LSCF0 cells were only 62 and 46 mW cm^{-2}, respectively. The ohmic resistance of the LSCF5 cell and the LSCF0 cell were both approximately 1.2 Ω cm^2, and the ohmic resistance of the LSCF10 was 1.3 Ω cm^2. The polarization impedance of the LSCF10 cell was approximately 0.63 Ω cm^2, which was smaller than that of the LSCF5 cell (1.1 Ω cm^2) and LSCF0 cell (1.6 Ω cm^2). According to previous research (Jayakumar et al. 2011), the polarization impedance of the LAA was approximately 0.06 Ω cm^2. Therefore, in the Nyquist diagrams, the two semicircles of each cell both come from the cathodes. The different performances of the button fuel cells indicated that the different amounts of pore former in the spraying powder influenced the polarization impedance of the cathode. The impedance data of LSCF0 show an obvious Warburg-type impedance, which suggests a scarcity of mass-transport channels in the cathode. The significant difference in the impedance data among the three cells is a result of the different amount of pore former in the sprayed powder. The sufficient mass transport in the LSCF10 cathode provides it with better performance than that of LSCF5 and LSCF0.

The cathodes of the button fuel cells were characterized by SEM after the electrochemical tests. Figure 4 (a) shows an SEM image of the cathode in the LSCF0 cell. The porosity of the cathode was very low, and it was difficult for air to diffuse through the cathode layer, resulting in a relatively significant Nernst diffusion impedance. Figure 4 (b) shows an SEM image of the cathode in the LSCF10 cell. The porosity of the cathode was increased by adding pore former to the spraying powder, and the diffusion impedance decreased accordingly. However, the high content of pore former in the spraying powder resulted in relatively poor contact between the cathode particles and led to an increase in ohmic impedance.

Figure 5 (a) and (b) show the polarization curves and EIS results, respectively, of the button fuel cells with the LSCF10 cathode and LSM10 cathode. The peak power density of the LSM10 cell was only 29 mW cm^{-2}, which was far less than that of the LSCF10 cell. However, the ohmic impedance of the LSM10 cell was much larger than that of the LSCF10 cell. This result can be attributed to the mixed electronic and ionic conductivities of the LSCF material (Zhang et al. 2016), and these mixed conductivities greatly expanded the reaction interface for oxygen reduction at the cathode of the cell. within contrast, the LSM material (T.Miruszewski et al. 2016) only conducts electrons at the working temperatures of SOFCs

The present LAA-SOFC with the LSCF10 cathode was compared with the plasma-sprayed SOFCs with different electrode arrangement type in Table 2. The polarization impedance of the cathode-down cells was much larger than that of the anode-down cells. In previous studies, the cathodes of the anode-down cells were prepared by a low torch power and a long spray distance, so the cathode particles were semi-molten when reaching the substrates. This made the plasma sprayed cathode layers porous but also decreased the bond strength of the cathode. For the cathodes of the anode-down cells, a low bond strength is generally acceptable because they were prepared at the outermost layer of the fuel cells and there wouldn't be any other spraying process after the cathodes were prepared. Considering to the extra complexity, the pore former was rarely used in cathode fabrication of the anode-down plasma-sprayed cells. However, for the cathode-down cells, if the bond strength of the cathodes was low, the heat and the impact causing by the plasma torch would make the coating crack or break off. Therefore, the cathodes were prepared with a relatively high torch power, which would result in a lower porosity and a larger polarization impedance. In the present research, with the pore former addition, the porosity and the performance of the cathode was improved.

Table 2

Comparison of the plasma-sprayed SOFCs with different electrode arrangement type.

Authors	Cathode Materials	Spraying Method	Type	Pore Former	Polarization Impedance at 750°C
Tsai et al. (2014)	LSCF-LSGM	Atmospheric plasma spraying	Anode-down	15 wt.% carbon black	0.128 Ω cm^2
Wang et al. (2020)	LSCF	Atmospheric plasma spraying	Anode-down	None	0.15 Ω cm^2
Harris et al. (2017)	LSCF-SDC	Atmospheric plasma spraying	Anode-down	25 wt.% carbon black	0.37 Ω cm^2
None	0.41 Ω cm^2				
Fan et al. (2016)	LSCF	Suspension plasma spraying	Symmetrical cell	0.3 wt.% carbon black	0.062 Ω cm^2
Waldbillig and Kesler (2011)	LSM-YSZ	Suspension plasma spraying	Cathode-down	None	0.75 Ω cm^2
Metcalfe et al. (2013)	LSCF-SDC	Atmospheric plasma spraying	Cathode-down	None	4.1 Ω cm^2
Anode-down	None	0.13 Ω cm^2			
Present Study	LSCF	Atmospheric plasma spraying	Cathode-down	10 wt.% carbon black	0.63 Ω cm^2

3.2 Performance of the Tubular LAA-SOFC

The tubular LAA-SOFC was fabricated with an LSCF10 cathode because of its respectable electrochemical performance in the button cell experiments. Figure 6 shows a cross-sectional SEM image of the tubular LAA-SOFC. The calculated reaction area of the tubular cell was 59.7 cm^2. Figure 7 shows the voltage of the tubular fuel cell during the 20-hour constant current test. The voltage decreased from 0.62 to approximately 0.55 V for the first 8 hours and remained stable for the following 12 hours. Figure 8 (a) and (b) show the polarization curves and EIS results, respectively, of the tubular cell measured before and after the test. The peak power of the tubular cell before the discharging test was approximately 2.5 W and decreased to approximately 1.8 W after the test. The decrease in the output power was mainly due to the increase in the ohmic impedance. The ohmic impedance increased significantly from 36 to 53 mΩ, and the polarization impedance increased slightly from 21 to 25 mΩ. According to the ex situ analysis, the increase in ohmic impedance was mainly caused by the oxidation of the threaded joint between the tubular cell and the air channel. The ohmic impedance of the tubular cell could be stabilized by optimizing the connection methods, such as welding.

The operating power density of the current tubular LAA-SOFC is relatively low (approximately 20.9 mW cm^{-2}). However, the LAA-SOFC showed an energy efficiency of 54.3% with the calculation method provided by Cao et al.(2019). In their calculation method, the energy efficiency of the LAA-SOFC is the product of the fuel efficiency, the theoretical efficiency and the voltage efficiency. Benefit from the solid state of the coal and the balance of the coal oxidation, the fuel efficiency of the Taixi coal in LAA was approximately 97% (Wang et al. 2014a). In regard to the theoretical efficiency, the heat requirement of the Sb_2O_3 reduction reaction could be provided by the Sb oxidation because of the large thermal capacity and the high thermal conductivity of the liquid antimony bath. Hence, the theoretical efficiency of the LAA-SOFC could be calculated by dividing the Gibbs free energy change of Sb oxidation (ΔG, −74.25 kJ per mol electron transfer at 1023 K) into the enthalpy change (ΔH, −98.66 kJ per mol electron transfer at 1023 K) of carbon oxidation in air, result in 75.3%. The cell operating voltage in the end of the 20-h constant current test was 0.55 V so the voltage efficiency was 74.3%. Considering the 1-kW LAA-SOFC stack with tubular cells in the present research, the size of the stack could be estimated. We assumed that the spacings between two adjacent cells were 1 cm and the utilized lengths of each tubular cell were 30 cm (the utilized length of the tubular cell was 7.6 cm in the present research). Thus, the size of the stack was 50×50×20 cm (196 tubular cells). Compared to that of other 1-kW fuel cell stacks by the APS method (approximately 15×15×30 cm, 25 planar cells, (Tsai et al. 2018)), the size of the as-prepared 1-kW fuel cell stack was relatively large. However, the tubular configuration could simplify the sealing of the stack. In addition, considering the space and cost saved by removing the purification equipment and the prospects of improving the LAA-SOFC performance, tubular LAA-SOFC stacks could be an attractive choice for converting solid carbon fuels.

Conclusions

In this paper, button LAA-SOFCs with different cathode materials and ratios of pore former were prepared by the APS method and measured at 750°C. The effect of the cathode structure on the electrochemical performance of the cathode-down SOFCs was evaluated. A high amount of pore former in the powder during cathode fabrication could decrease the polarization impedance of the cathode but would increase the ohmic impedance. An optimized spraying method for LAA-SOFCs was developed. A tubular LAA-SOFC was prepared by the APS method based on the optimized method and reached a peak power of 2.5 W. The tubular cell was also measured at a constant current of 2 A for 20 hours and was fed sulfur-containing coal to demonstrate its impurity resistance and electrode stability.

Acknowledgment

This work was supported by the National Key R&D Program of China (2018YFB0905602), the Huaneng Group Science and Technology Research Project (HNKJ20-H50), the Beijing Natural Science Foundation Outstanding Youth Science Foundation Project (JQ18009), the National High Level Talents Special Support Plan and the Tsinghua University Initiative Scientific Research Program.

References

1. Cao T, Huang K, Shi Y, Cai N (2017) Recent advances in high-temperature carbon–air fuel cells Energy & Environmental Science 10:460-490 doi:10.1039/c6ee03462d
2. Cao T, Huang K, Shi Y, Cai N (2018) Plasma-spray derived, corrosion-resistive electrolyte for liquid antimony anode direct carbon fuel cell Journal of Power Sources 403:76-81 doi:10.1016/j.jpowsour.2018.09.036
3. Cao T, Song P, Shi Y, Ghoniem AF, Cai N (2019) Oxy-combustion of coal in liquid-antimony-anode solid oxide fuel cell system Proceedings of the Combustion Institute 37:2841-2848 doi:10.1016/j.proci.2018.08.056
4. Dong B, Li C, Liu C, Huang B, Wang Q, Fan W, Li P (2019) Integrated gasification fuel cell power generation technology with CO2 near zero emission and its challenges Coal Science and Technology 47:189-193
5. Duan N-Q, Cao Y, Hua B, Chi B, Pu J, Luo J, Jian L (2016) Tubular direct carbon solid oxide fuel cells with molten antimony anode and refueling feasibility Energy 95:274-278 doi:10.1016/j.energy.2015.10.033
6. Fan ESC, Kuhn J, Kesler O (2016) Suspension plasma spraying of La0.6Sr0.4Co0.2Fe0.8O3−δ cathodes: Influence of carbon black pore former on performance and degradation Journal of Power Sources 316:72-84 doi:10.1016/j.jpowsour.2016.02.075
7. Fan H, Han M (2014) Electrochemical performance and stability of Sr-doped LaMnO3-infiltrated yttria stabilized zirconia oxygen electrode for reversible solid oxide fuel cells International Journal of Coal Science Technology 1:56-61
8. Harris J, Kuhn J, Kesler O (2017) Atmospheric Plasma-Sprayed Metal-Supported Solid Oxide Fuel Cells with Varying Cathode Microstructures Journal of The Electrochemical Society 164:F441-F447 doi:10.1149/2.1591704jes
9. Henne R (2007) Solid Oxide Fuel Cells: A Challenge for Plasma Deposition Processes Journal of Thermal Spray Technology 16:381-403 doi:10.1007/s11666-007-9053-4
10. Javadekar A, Jayakumar A, Pujara R, Vohs JM, Gorte RJ (2012) Molten silver as a direct carbon fuel cell anode Journal of Power Sources 214:239-243 doi:10.1016/j.jpowsour.2012.04.096
11. Jayakumar A, Javadekar A, Gissinger J, Vohs JM, Huber GW, Gorte RJ (2013) The stability of direct carbon fuel cells with molten Sb and Sb-Bi alloy anodes AIChE Journal 59:3342-3348 doi:10.1002/aic.13965
12. Jayakumar A, Küngas R, Roy S, Javadekar A, Buttrey DJ, Vohs JM, Gorte RJ (2011) A direct carbon fuel cell with a molten antimony anode Energy & Environmental Science 4:4133-4137 doi:10.1039/c1ee01863a
13. Jayakumar A, S. Lee, A. Hornés, Vohs JM, Gorte RJ (2010) A Comparison of Molten Sn and Bi for Solid Oxide Fuel Cell Anodes Journal of The Electrochemical Society 157:B365-B369

14. Jiang Y, Cao T, Shi Y, Cai N (2019) Sulfur-resistant Liquid Antimony Anode for Direct Carbon Fuel Cells ECS Transactions 1:2001-2010 doi:10.1149/09101.2001ecst
15. Jiang Y, Cao T, Shi Y, Cai N (2020) Liquid Antimony Anode for Converting Sulfur-Containing Coal in Direct Carbon Fuel Cells Journal of The Electrochemical Society 167 doi:10.1149/1945-7111/ab8bfb
16. Li H, Yu Yu, Han M, Lei Z (2014) Simulation of coal char gasification using O2/CO2 International Journal of Coal Science Technology 1:81-87
17. Li M, D.Rao A, Brouwer J, ScottSamuelsen G (2010) Design of highly efficient coal-based integrated gasification fuel cell power plants Journal of Power Sources 195:5707-5718
18. Ma J et al. (2019) Hot corrosion of yttria-stabilized zirconia by liquid antimony and antimony oxide Journal of power sources 434:226764
19. Metcalfe C, Harris J, Kuhn J, Marr M, Kesler O (2013) Progress in Metal-Supported Axial-Injection Plasma Sprayed Solid Oxide Fuel Cells Using Nanostructured NiO-Y0.15Zr0.85O1.925 Dry Powder Anode Feedstock Journal of Thermal Spray Technology 22:599-608 doi:10.1007/s11666-013-9884-0
20. T.Miruszewski, J.Karczewski, B.Bochentyn, P.Jasinski, M.Gazda, B.Kusz (2016) Determination of the ionic conductivity of Sr-doped lanthanum manganite by modified Hebb-Wagner technique Journal of Physics Chemistry of Solids 91:163-169 doi:https://doi.org/10.1016/j.jpcs.2016.01.005
21. Tao T, Bateman L, Bentley J, Slaney M (2007) Liquid Tin Anode Solid Oxide Fuel Cell for Direct Carbonaceous Fuel Conversion Ecs Transactions 5:115-124
22. Tsai CH, Hwang CS, Chang CL, Nien SH, Chuang CM, Chuang Shie ZY (2014) The Effect of Plasma Spraying Power on La0.58Sr0.4Co0.2Fe0.8O3-δ-La0.8Sr0.2Ga0.8Mg0.2O3-δComposite Cathode Interlayer Microstructure and Cell Performance Fuel Cells 14:83-90 doi:10.1002/fuce.201300143
23. Tsai CH et al. (2018) Performances of Plasma Sprayed Metal-supported Solid Oxide Fuel Cell and Stack Fuel Cells 18:800-808 doi:10.1002/fuce.201800080
24. Waldbillig D, Kesler O (2011) Electrochemical testing of suspension plasma sprayed solid oxide fuel cell electrolytes Journal of Power Sources 196:5423-5431 doi:10.1016/j.jpowsour.2011.02.057
25. Wall TF (2005) Oxy-fuel combustion technology for coal-fired power generation Progress in Energy Combustion Science 31:283-307
26. Wang H, Cao T, Shi Y, Cai N, Yuan W (2014a) Liquid antimony anode direct carbon fuel cell fueled with mass-produced de-ash coal Energy 75:555-559 doi:10.1016/j.energy.2014.08.017
27. Wang H, Shi Y, Cai N (2013) Effects of interface roughness on a liquid-Sb-anode solid oxide fuel cell International Journal of Hydrogen Energy 38:15379-15387 doi:10.1016/j.ijhydene.2013.09.134
28. Wang H, Shi Y, Cai N (2014b) Characteristics of liquid stannum anode fuel cell operated in battery mode and CO/H2/carbon fuel mode Journal of Power Sources 246:204-212 doi:10.1016/j.jpowsour.2013.07.085
29. Wang H, Shi Y, Cai N (2014c) Polarization characteristics of liquid antimony anode with smooth single-crystal solid oxide electrolyte Journal of Power Sources 245:164-170 doi:10.1016/j.jpowsour.2013.06.125

30. Wang Y-p, Gao J-t, Chen W, Li C-x, Zhang S-l, Yang G-j, Li C-j (2020) Development of ScSZ Electrolyte by Very Low Pressure Plasma Spraying for High-Performance Metal-Supported SOFCs Journal of Thermal Spray Technology 29:223-231 doi:10.1007/s11666-019-00970-1
31. Zhang S-L et al. (2017) Thermally Sprayed Large Tubular Solid Oxide Fuel Cells and Its Stack: Geometry Optimization, Preparation, and Performance Journal of Thermal Spray Technology 26:441-455 doi:10.1007/s11666-016-0506-5
32. Zhang S-L et al. (2016) Thermally sprayed high-performance porous metal-supported solid oxide fuel cells with nanostructured La0.6Sr0.4Co0.2Fe0.8O3−δ cathodes Journal of Materials Chemistry A 4:7461-7468 doi:10.1039/c6ta02065h

Figures

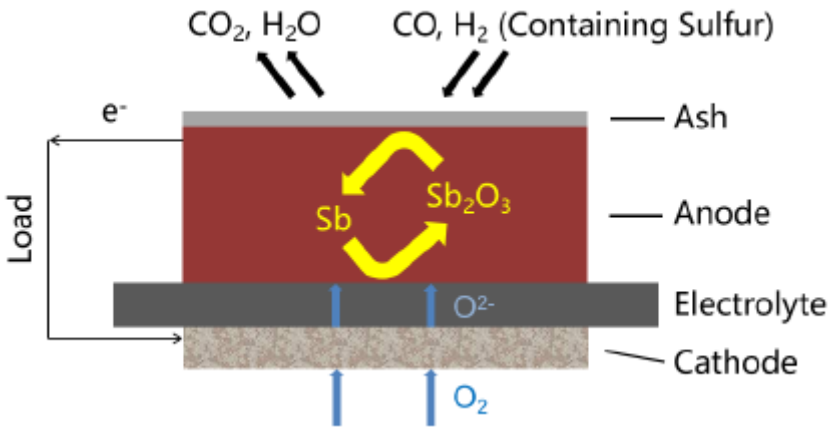

Figure 1

Working principle of the liquid antimony anodes.

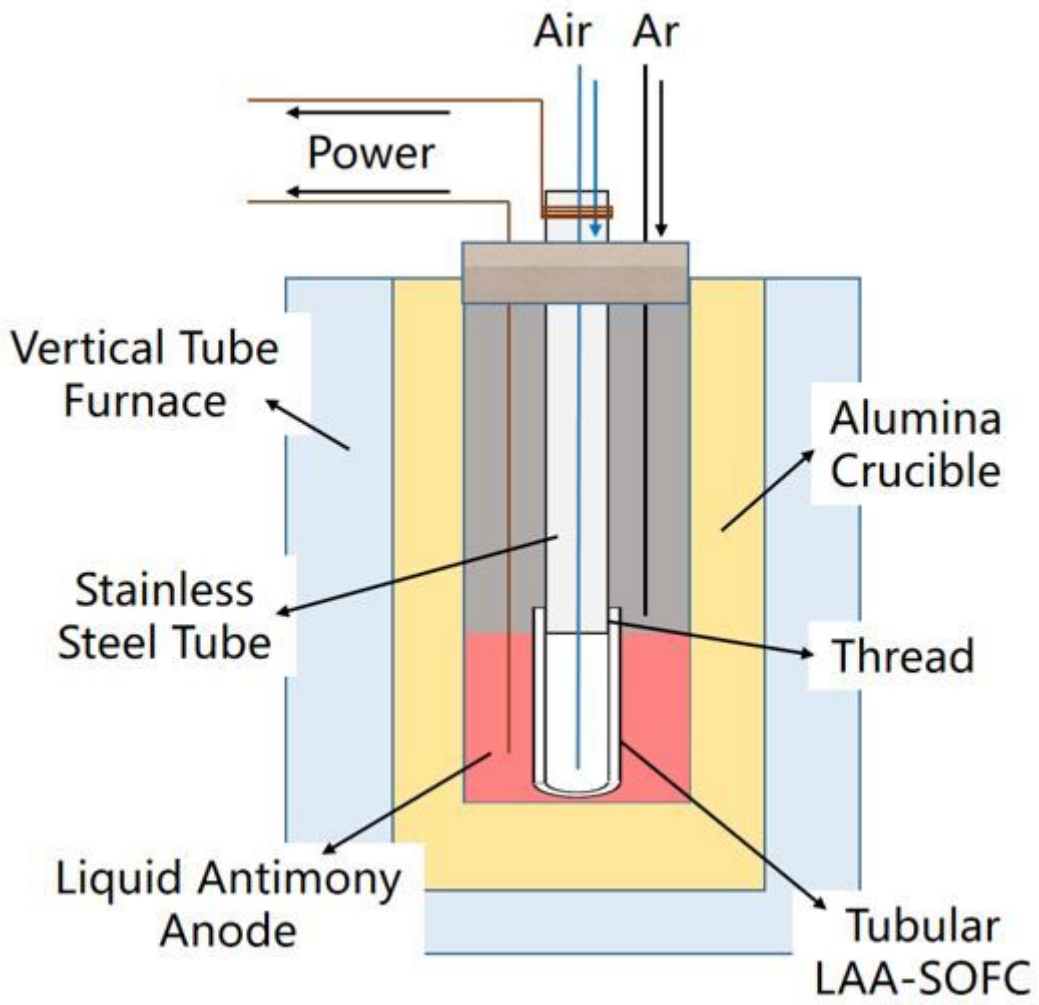

Figure 2

Electrochemical testing setup for the sprayed tubular LAA-SOFC.

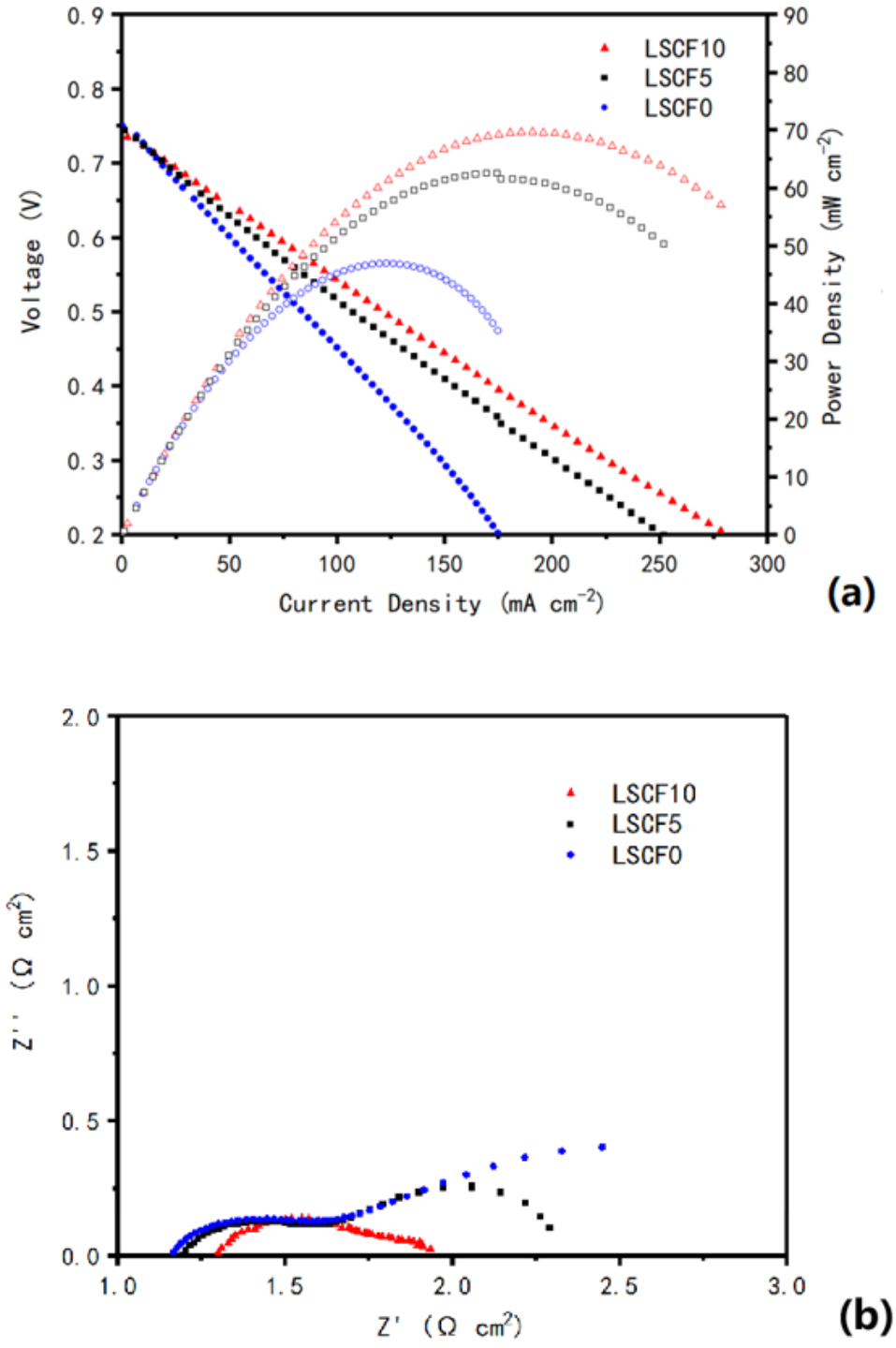

Figure 3

Polarization curves (a) and EIS results (b) of LSCF cathode button fuel cells with different amounts of pore former.

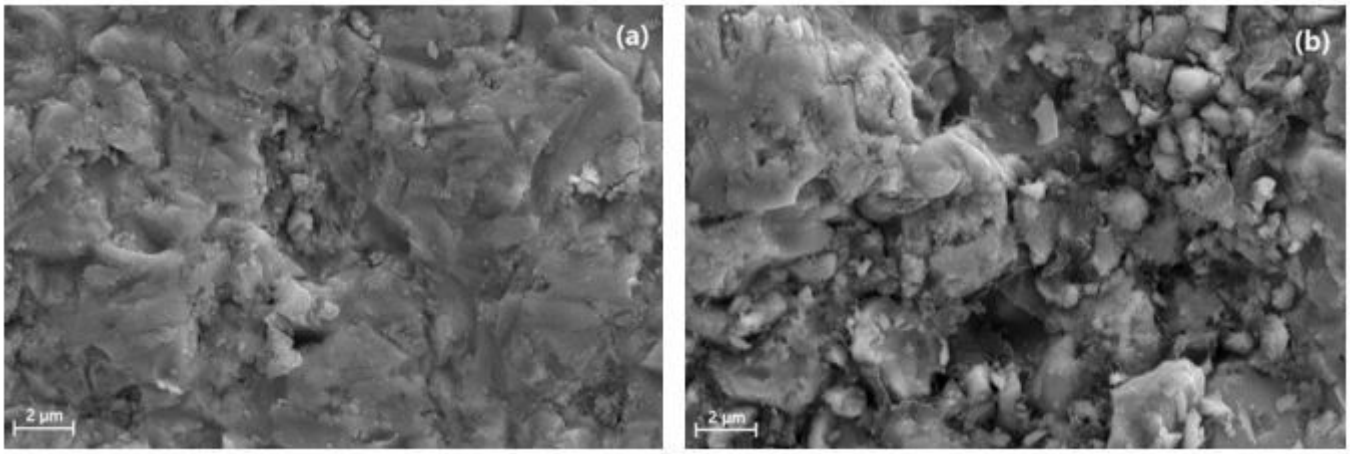

Figure 4

SEM images of the cathode in the LSCF0 (a) and LSCF10 cells (b).

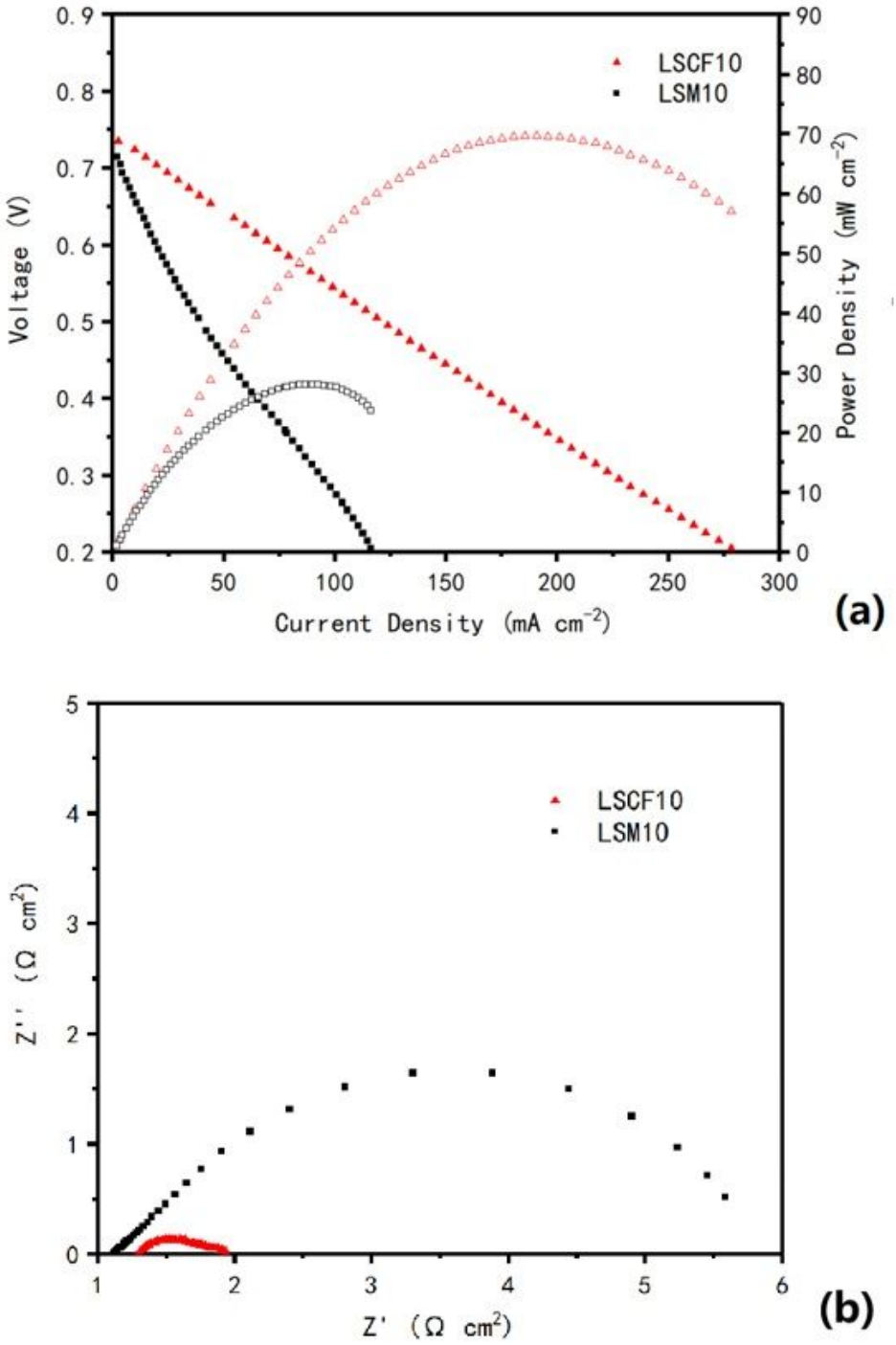

Figure 5

Polarization curves (a) and EIS results (b) of the button fuel cells with the LSCF10 and LSM10 cathodes.

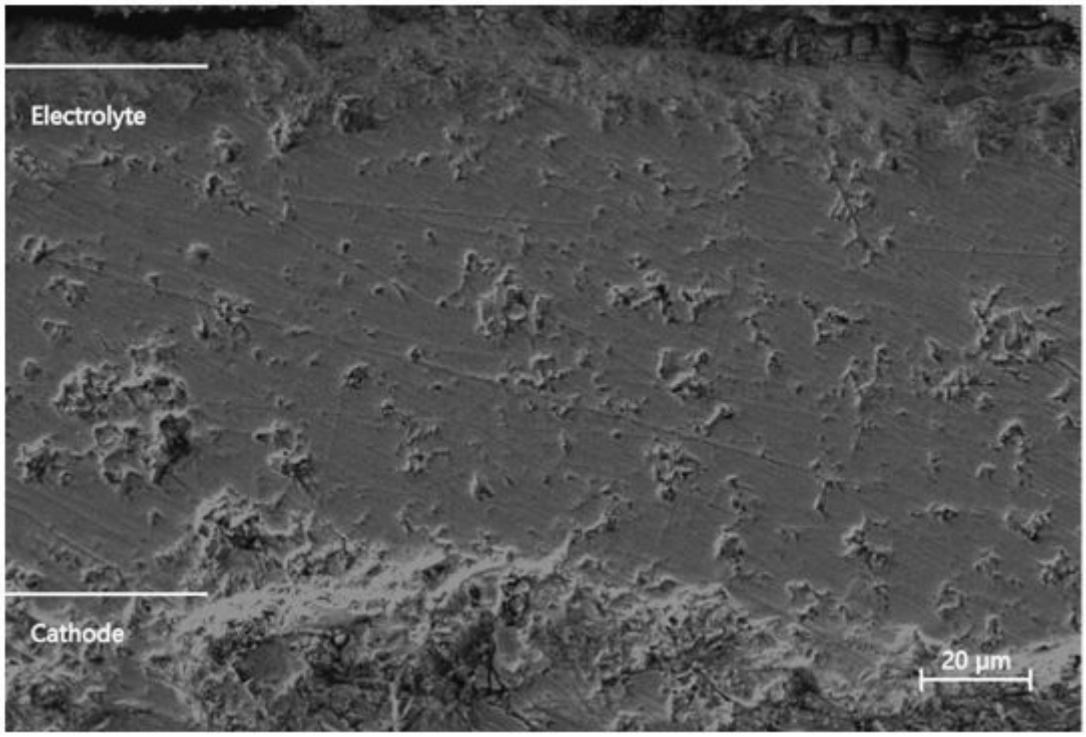

Figure 6

Cross-sectional SEM image of the tubular LAA-SOFC.

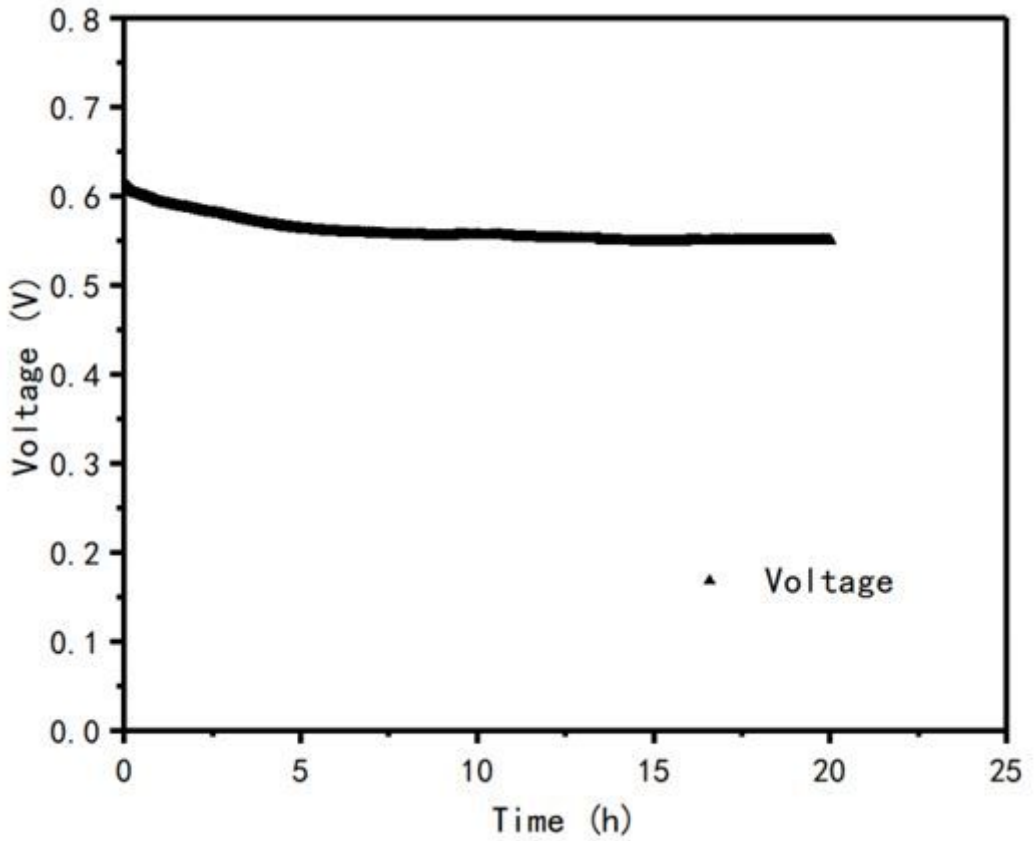

Figure 7

Voltage of the tubular fuel cell during the 20-hour constant current test.

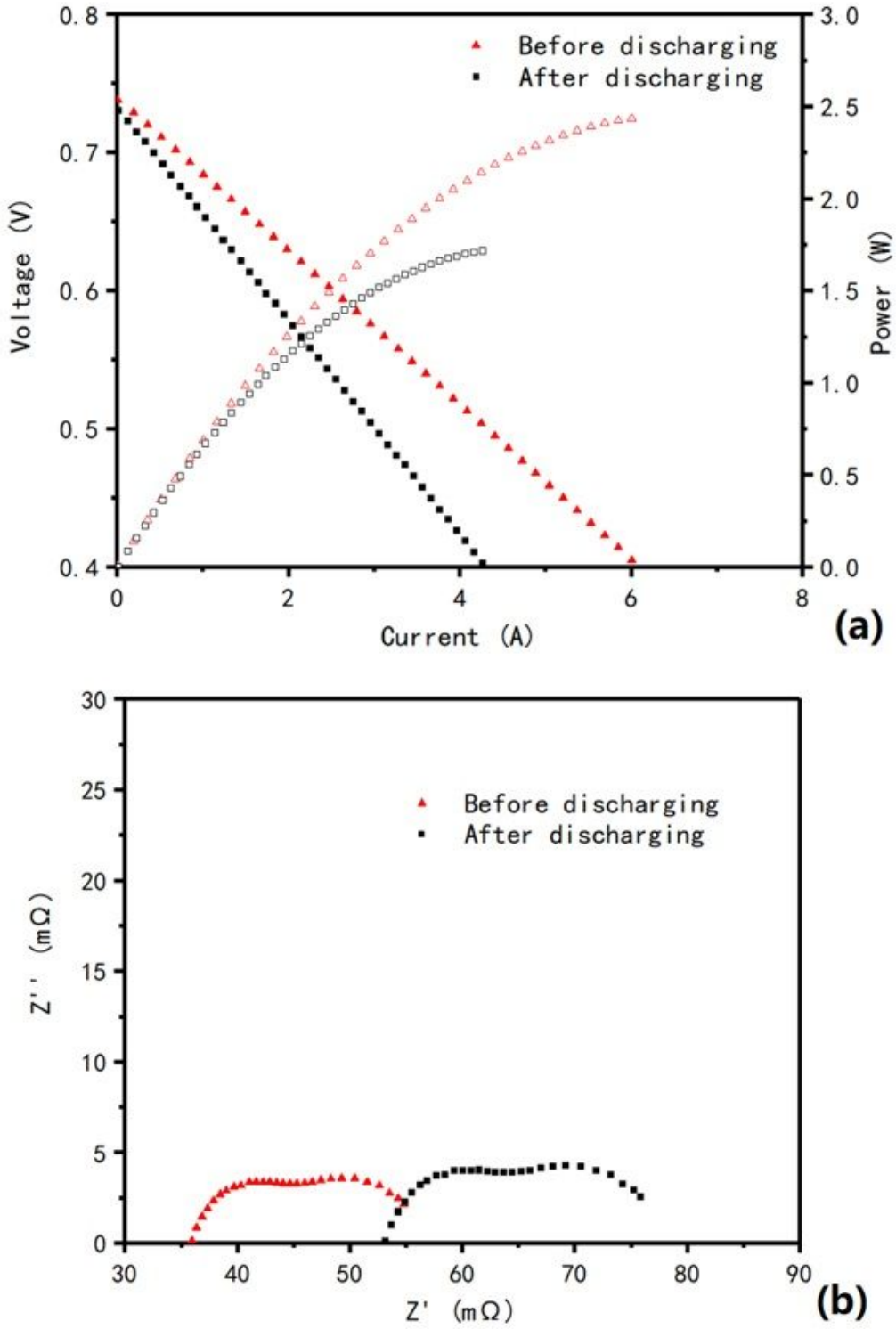

Figure 8

Polarization curves (a) and EIS results (b) of the tubular LAA-SOFC measured before and after the constant current test.

Supplementary Files

This is a list of supplementary files associated with this preprint. Click to download.

- equations.docx